Available online at www.sciencedirect.com
SCIENCE DIRECT®

NUCLEAR
SCIENCE
AND
TECHNIQUES

Nuclear Science and Techniques, Vol.17, No.4 (2006) 202–211

Probing Co/Si interface behaviour by X-ray photoelectron spectroscopy (XPS) and atomic force microscopy (AFM)

PAN J. S.[1,*] LIU R. S.[2] TOK E. S.[1,2]

(*[1]Institute of Materials Research and Engineering, 3 Research Link, Singapore 117602;*
[2]Department of Physics, National University of Singapore, Kent Ridge, Singapore 119260)

Abstract In this work, we investigate the Co-Si reaction, the Co growth mode at room temperature, diffusion behaviour as well as morphology evolution during annealing on both H-terminated and clean Si(001) and Si(111) surfaces. From in-situ X-ray photoelectron spectroscopy (XPS) investigation, "Co-Si" reaction appears to occur on both H-terminated and clean surfaces at room temperature (RT) and the silicide crystallinity is improved upon annealing. Co growth mode on H-terminated Si surfaces occurs in a pseudo layer-by-layer manner while small close-packed island growth mode is observed on the clean Si surface. Upon annealing at different temperatures, Co atom concentration decreases versus annealing time, which in part is attributed to Co atoms inward diffusion. The diffusion behaviour on both types of surfaces demonstrates a similar trend. Morphology study using ex-situ atomic force microscopy (AFM) shows that the islands formed on Si(001) surface after annealing at 700 °C are elongated with growth directions alternate between the two perpendicular $[\bar{1}10]$ and [110] directions. Triangular islands are observed on Si (111) surface.

Key words Cobalt, Silicon, Metal-semiconductor interfacial reaction, Hydrogen termination, Growth mode, Diffusion, Surface morphology, XPS, AFM

CLC numbers TN304.2$^+$4, TH744.11$^+$2, TH742.9

1 Introduction

The importance of studying the behaviour of transition metal overlayers on Si surfaces stems from its technological application as silicides in integrated circuit technology. In particular, the fabrication of defect-free $CoSi_2$ films with well-defined surfaces and abrupt interfaces has received tremendous attention because of their low resistivity, high thermal stability and long electron mean free path properties [1, 2]. These properties improve the performance of device applications such as Schottky barriers, ohmic contacts, interconnections and low resistivity gates. In addition, $CoSi_2$ can also be epitaxially grown on a silicon substrate. It belongs to the cubic crystal system and has a close lattice match with silicon (mismatch ~1.2%), thus making $CoSi_2$ a potential candidate in ultra-large-scale integration (ULSI) device fabrication [3, 4]. Several techniques ranging from molecular beam epitaxy (MBE), reactive deposition epitaxy (RDE) and solid-phase epitaxy (SPE) have been used to fabricate these $CoSi_2$ thin films [5]. In MBE, Co metal and silicon are co-evaporated onto a Si substrate held at an elevated temperature, usually between 400°C and 600°C. In RDE, Co is directly deposited on a heated silicon substrate. Unlike MBE or RDE, SPE is a two-step process. A thick Co metal film (ranging from a few tens of nanometers to micrometers) is first deposited at room temperature on a clean Si surface.

---

[*] Corresponding author, e-mail: js-pan@imre.a-star.edu.sg

Received date: 2006-07-20

This is followed by annealing at an elevated temperature to allow Co and Si to react and form the silicide film. A variety of techniques ranging from transmission electron microscopy (TEM), X-ray diffraction (XRD), X-ray photoelectron spectroscopy (XPS), Auger electron spectroscopy (AES) and ultraviolet photoelectron spectroscopy (UPS) have been used to characterise the behaviour of these Co layers on Si substrates, in particular, Co deposition and annealing on clean Si(111) surfaces [6-9]. The reaction of Co and Si to form $CoSi_2$ can be summarised as follows. The formation of a particular Co-Si phase is temperature dependent and it is believed to occur through the following stages:

$$\mathrm{Co} \xrightarrow{\sim 250°\mathrm{C}} \mathrm{Co_2Si} \xrightarrow{\sim 350°\mathrm{C}} \mathrm{CoSi} \xrightarrow{\sim 650°\mathrm{C}} \mathrm{CoSi_2}$$

A cobalt rich Co_2Si phase is formed at ~ 250°C. This phase, however, is not stable at higher temperatures and further annealing to ~350°C leads to the formation of a highly resistive CoSi phase. By annealing to higher temperatures, a silicon rich, low resistive $CoSi_2$ phase forms at ~ 650°C [10].

Recently, growth of Co on H-terminated Si surfaces has also been a subject of great interest. The reason for incorporating H-termination is to terminate the reactive dangling bonds found on the clean surfaces. It has been reported that the adsorption of hydrogen and termination of the silicon dangling bonds can alter surface energy, adatom diffusion, segregation and nucleation behaviour, resulting in the modification of the epitaxial film produced [11]. In fact, the growth and structure of thin metal films on H-terminated Si surfaces have been investigated for a great variety of metals such as the 3d-transition metals, e.g. Ti, Fe and Ni [12, 13], the noble metals, e.g. Cu, Ag and Au [14-16], and the trivalent simple metals such as Al and In [17-19]. For example, Murano *et al.* [12] described a "surfactant effect" of hydrogen for nickel growth on Si (7×7) surface. On a clean surface, they found that 2-monolayers (ML) of Ni can grow in a layer-by-layer growth mode but change to 3-dimensional Stranski-Krastanove mode after that. However, when Ni was deposited on H-terminated surface, 7 ML of Ni can now be deposited on this surface in a layer-by-layer growth mode. The implication is that hydrogen termination of Si dangling bonds enhances the surface diffusion length, thereby modifies the growth mode from three dimensional to two dimensional. Shen *et al.* [17] also found dramatic differences between Al island nucleation on bare and monohydride Si(001) surface. Their studies revealed that individual Al atom can diffuse over relatively large distances on H-terminated surface before colliding to form immobilized Al clusters. The diffusion length of Al adatoms is much smaller on bare Si, due to rapid Al-Si bonding and formation of stable ad-dimers. In addition, hydrogen termination at the Al/H-Si (111) interface also suppressed the formation of interfacial AlSi which promoted island growth [19]. Hydrogen termination of the surface dangling bonds of Si may similarly prevent direct reaction between Co and Si dangling bonds and in the process modify the growth behavior and improve various film characteristics (growth mode, interfacial roughness and/or surface roughness). In this respect, there is again no lack of consensus in the literature. Palasantzas *et al.* [20] investigated the behaviour of Co on H-terminated Si (001) surfaces by scanning tunneling microscopy (STM). They claimed that due to the absence of nucleation sites for silicide formation, the nucleation and growth mode were dominated by the formation of non-epitaxial islands which merged by increasing Co coverage. This observation was also reported by Copel *et al.* [21] but on Si(111) surface instead. However more recently studies inferred from a STM study showed formation of dense granular Co films observed on H/Si(111)1×1 surface [22] and island growth mode occurs instead. XRD [22] measurements by the same authors revealed that H-terminated Si(111) substrates appear to enable film growth with single crystalline surface orientation for Fe, Co, and Ni metals. However, in sharp contrast to the growth of Co on clean Si surfaces, there are relatively few reported works on the study of the Co behaviour on H-terminated Si surfaces.

For these reasons, it is certainly of interest in this paper to resolve the growth of Co on these H-terminated Si surfaces and compare it with the results obtained on a clean surface. We therefore contribute to this area of work by presenting a systematic investigation of the growth of Co on both H-terminated and clean Si(001) and Si(111) surfaces, followed by annealing to different temperatures. We will use XPS to identify the chemical bonds of reaction products and to determine growth modes. The surface morphology will be imaged by atomic force microscopy (AFM). Except for AFM observation, all the experiments were performed in-situ under an ultra-high vacuum (UHV) condition. We will show that (i) formation of an initial $CoSi_2$ – like phase first occurs on both clean and H-terminated surfaces; (ii) a pseudo layer-by-layer growth mode occurs on H-terminated Si surfaces and closed-packed small island growth mode occurs on clean Si surfaces; (iii) formation of a metallic Co film on top of an initial $CoSi_2$ layer on both clean and H-terminated surfaces as Co coverage increases; (iv) the mechanism governing the silicide reaction for very thin deposited Co layers; (v) Co diffusion behaviour on both clean and H-terminated surfaces at different annealing temperatures; and (vi) formation of rectangular islands on Si(001) substrates while triangular islands on Si(111) substrates.

2 Experimental

Hydrophophic hydrogen-terminated boron-doped Si(001) and Si(111) samples with resistivity of 25±10 Ω·cm were prepared by using a modified RCA wet chemical cleaning method with a final HF dip. VLSI grade HF and $NH_4OH/H_2O_2/H_2O$ solution were used to remove surface oxides and carbon, and at the same time passivate the surface with hydrogen before introduction into a UHV system, kept under a pressure of 1×10^{-8} Pa. This method of preparation is known to produce a hydrophobic H-terminated Si surface and is stable in the UHV. Heating the surface beyond 300°C leads to desorption of hydrogen and formation of a bare Si surface and in the present study the preparation of bare Si surface was done by annealing the H-terminated Si surface to 550°C-600°C for 30 min. A cobalt e-beam evaporator was used to deposit Co onto the Si surface at a rate of ~ 0.6 $ML{\cdot}min^{-1}$, during which the pressure was maintained at ~0.1μPa. In-situ sample annealing was done using resistive heating. The sample temperature was monitored with a thermocouple directly in contact with the sample. The XPS experiments were performed using a VG ESCALAB 220i-XL instrument equipped with a monochromatic Al *K*α (1486.7 eV photons) and an unmonochromated Mg *K*α X-ray source (1253.6 eV photons), a concentric hemispherical analyzer and a magnetic immersion lens (XL lens) to increase the sensitivity of the instrument. The instrument was calibrated with pure gold, silver and copper standard samples by setting the Au $4f_{7/2}$, Ag $3d_{5/2}$ and Cu $2p_{3/2}$ peaks at binding energies of 83.98±0.02 eV, 368.26±0.02 eV and 932.67±0.02 eV respectively. All spectra were recorded in the constant pass energy mode of the analyzer using a monochromatic Al *K*α X-ray source. Survey spectra were recorded with a pass energy of 150 eV and a 1 eV step width. Co $2p_{3/2}$, Si 2p and C 1s high-resolution spectra were recorded with a pass energy of 20 eV and 0.1 eV step width. After a Shirley-type background subtraction, an XPS spectral deconvolution was achieved by a curve-fitting procedure based on Lorentzians broadened by a Gaussian, due to the instrumental resolution, using the manufacturer's standard software. Component peak shape and full-widths-at-half-maximums (FWHMs) for a particular peak envelope were kept the same during curve fitting. Quantification was done using relative sensitivity factors (RSFs) for our instrument, which take into consideration both the corresponding photoionization cross-sections of Scofield and the transmission function of the spectrometer. The surface morphologies of the surface were imaged in Tapping Mode using a Digital Instruments D3000 atomic force microscope (AFM).

3 Results and discussion

3.1 Co/Si reaction on the H-terminated and clean Si surfaces at various temperatures

Fig. 1(a) shows the typical Co $2p_{2/3}$ versus Co coverage on clean or H-terminated Si(111) surface at room temperature (RT). In the initial stages of Co deposition, the Co $2p_{3/2}$ peak is observed at a binding energy of 778.7 ± 0.1 eV, which is about 0.5 eV shift from that of pure Co $2p_{3/2}$ peak (778.2 ± 0.1 eV). This value is very close to that of bulk $CoSi_2$ (778.8 ± 0.1 eV). With increasing coverage, the binding energy of Co $2p_{2/3}$ shifts gradually towards the value as expected for bulk Co film. Identical XPS spectra evolution were also observed for Co deposition on clean and H-terminated Si(001) surfaces.

At low metal coverages, a shift in the binding energy (BE) to a higher value away from the bulk core levels value has previously been observed in growth of Ir, Pd, Au, Cu and Al on graphite surfaces [23-25] as well as Cu on TiO_2 [25, 26]. In these systems, the shift in BE has been attributed to be a consequence of incomplete screening of the final electronic (hole) state, which is usually the case if small clusters are formed (cluster effect) [27, 28]. In the present study, the shift to a higher binding energy observed on both Si(111) and Si(001) surfaces at low Co coverage is unlikely to be attributed to the cluster effect. The surface morphology of Co deposited on H-terminated Si(111) surface as seen from Fig. 3 is still relatively smooth and no clusters were observed to be formed on the Si surfaces. Given that the value is very close to that of bulk $CoSi_2$ (778.8 ± 0.1 eV), we attribute this to the formation of a Co silicide phase and this occurs on both clean and H-terminated Si(001) and Si(111) surfaces. The formation of Co-Si bond on clean Si surfaces is perhaps not unexpected since there is the presence of unsatisfied Si dangling bonds at the surface. However, it is more difficult to apply this reasoning to the observation of a Co/Si reaction and formation of a Co-Si bond on a H-terminated Si surfaces since all the dangling bonds are now passivated. In this case, there are no available reactive Si dangling bonds to facilitate direct bond formation between Co and surface Si atoms. For this reaction to occur would imply a reaction between Co and the Si-H bond or with the Si-back bonding at the Si-Si-H surface. The interstitial model as proposed in Ref. [9] for growth on clean Si surfaces may help to explain how the Co silicide reaction can take place at RT on both clean and H-terminated surfaces. In the initial deposition stage, Co atoms can incorporate into the interstitials sites of the Si host lattice. The consequence of forming metal interstitials in Si is the weakening of the Si-Si covalent bond. Electrons in the neighboring Si-Si covalent bonds will no longer remain in their localized states and will have to share between the interstitial and Si atoms. This can result in the formation of a Co-Si bond at the growth front of Co/Si or Co/H-Si surfaces.

Experimentally, we observed that the binding energy of 778.7 ± 0.1 eV at Co coverage of 1% is very close to the value associated with bulk $CoSi_2$ (778.8 ± 0.1 eV). Given the limited mobility of adatoms at room temperature, the structure thus formed would likely be different from the equilibrium stable CaF_2-type $CoSi_2$ structure. We therefore described this phase as a “$CoSi_2$-like” film. Our results showed that silicide reaction can occur spontaneously at RT and low Co coverage of ~ 1% Co with respect to Si. More importantly with increasing Co coverage, the binding energy progressively moves to the signature of a metallic film. The implication is that this reaction only occurs at the initial Co/Si or Co/H-Si-Si interface and thereafter a metallic film grows above it. Our results for clean surfaces thus agree with previous work described in Refs. [6, 7, 29-32]. It is also known that hydrogen desorption from the Si surface is only significant above 300°C, and that the Si-H bond is particularly strong with a bond energy of 3.5 eV compared to the Si-Si bond energy of 2.3 eV [33]. Therefore, we infer that the silicide phase thus formed is most likely also H-terminated. Unlike clean surfaces, further deposition of Co at RT will therefore occur above a H-terminated silicide layer instead. Irrespectively, we therefore have growth of metallic cobalt on an initial silicide layer on both clean and H-terminated surfaces as Co coverage increases. The existence of the hydrogen atoms at Co/H-$CoSi_2$ interface may subsequently have an effect on the diffusion and nucleation behavior of subsequent deposited Co adatoms. This in turn may lead to a different surface morphology compared to the clean surface which will be discussed in the next section.

Fig. 1 (b) shows the typical Co $2p_{3/2}$ spectra obtained for different samples prepared by first depositing ~5 Å Co on clean or H-terminated Si(001) surface at RT followed by heating to different substrate temperatures each time. The room temperature spectrum shows that the binding energy of the Co $2p_{3/2}$ at 778.7 ± 0.1 eV, indicating the formation of a "Co-Si_2-like" overlayer on both clean and H-terminated silicon substrates as discussed above. The peak shape however is more asymmetric and more akin to a metallic-like Co environment. Annealing the sample beyond 100°C results in a shift in the binding energy of the Co $2p_{3/2}$ peak to 778.8 ± 0.1 eV, a value corresponding to Co in the bulk $CoSi_2$ crystal structure. It should be noted that the full width at half maximum

(FWHM) decreases from ~1.0 eV to ~0.8 eV with increasing temperatures. This decrease in the FWHM coupled with the change of the Co $2p_{3/2}$ peak shape from an asymmetric (metallic-like phase) to a symmetric shape (silicide phase), indicates the improvement of the silicide crystallinity and character. Identical XPS spectra were also obtained for Co deposited on clean and H-terminated Si(111) surfaces.

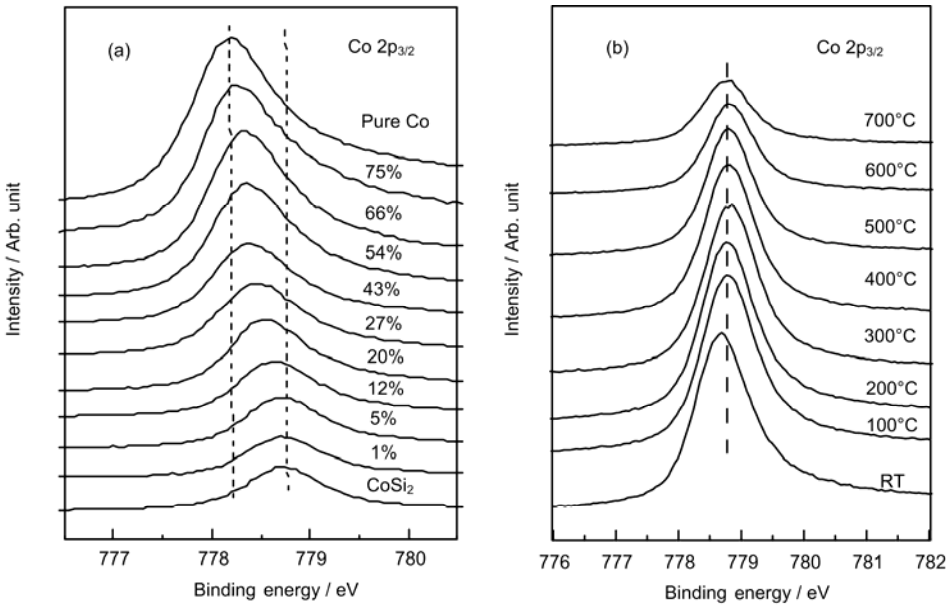

Fig.1 (a) The Co $2p_{3/2}$ spectra obtained from Co deposited H-terminated Si(111) surfaces at room temperature with increasing Co coverage. In comparison, Co $2p_{2/3}$ spectra from bulk Co and $CoSi_2$, were included. (b) The Co $2p_{3/2}$ spectra collected during annealing at different temperatures after depositing ~5% Co on the H-terminated Si(001) surface at room temperature.

As mentioned in the introduction, for Co thin films with conventional (1000 Å) thickness deposited on Si substrate, a sequence of stable phases $Co \rightarrow Co_2Si$ (~250°C) $\rightarrow CoSi$ (~350°C) $\rightarrow CoSi_2$ (~650°C) is observed with “formation temperatures” as shown in parentheses [10]. The metal rich silicides form by diffusion limited kinetics (metal species moving) with activation energies of ~2 eV, while $CoSi_2$ forms with nucleation limited kinetics. The same sequence is generally observed in very thin (50 Å) films under UHV conditions although the formation temperatures are generally lower [34]. However, for ultrathin (~5 Å) films, we cannot find such clear reaction sequence during annealing. A simple reason is that there may be not enough amount of Co atoms to form a Co rich silicide for ultrathin Co films on Si substrate.

3.2 The growth modes of Co on H-terminated and clean Si surfaces

A standard method for the determination of growth mode using XPS is to measure the adsorbate and the substrate signals while increasing the exposure of the overlayer metal. The S-*t* plots (electron spectroscopy signal versus evaporation time) should have a characteristic shape depending on the growth mode of the adsorbate metal. In case of layer-by-layer growth (FM growth), in which growth of a new atomic layer does not start until the preceding layer is complete, the S-*t* curve consists of a series of linear segments of decreasing gradient. The ‘break points’ (where each linear segment intersects) correspond to the completion of each monolayer. The growth occurs in the form of three-dimensional crystallites (Vollmer-Weber growth, VW), which should give the substrate and adsorbate signal intensities a slow rate of decay and increase respectively because large areas of the substrate remain clear of adsorbed material. Finally, Stranski-Krastanov (SK) growth falls midway between these two cases. Depending on the critical coverage, the S-*t* plot will consist of one or more linear segments followed by a slower decay/increase related to the formation and growth of islands.

Fig. 2 shows the evolution of the atomic fraction of Si (Si 2p) and Co (Co $2p_{3/2}$) as a function of Co-deposition time on both H-terminated Si(001) and

Si(111) surface at room temperature. Also shown in the plots are data collected when the same experiments were repeated on a graphite surface. The magnitude change in the signal (increase or decrease) with time is clearly much larger than the signals obtained from the graphite surface. The C 1s and Co $2p_{3/2}$ signals show a slow rate of decay and increase respectively. This is a characteristic of the Volmer-Weber growth mode. The XPS behaviour for growth of Co on H-terminated Si(001) or Si(111) surface is clearly different and it clearly does not follow the Volmer-Weber growth mode. The plots obtained on the H-terminated silicon substrates appear to be exponential-like. Although not shown here, the evolution of the atomic fraction of Si (Si 2p) and Co (Co $2p_{3/2}$) as a function of Co-deposition time on both clean Si(001) and Si(111) surfaces at RT shows no significant difference. The implication is that we have layer-by-layer growth mode on both clean and H-terminated Si surfaces. There is however no distinctive series of linear breaks as would be expected from an "ideal" layer-by-layer growth mode. There are several possible reasons for this observation: (a) It may be related to the silicide reaction which occurs upon deposition of Co on Si surfaces and the intermixing of two components resulting in silicide formation. This may cause the XPS signals to be different from the values calculated according to an ideal sharp unreacted interface model. (b) Growth occurs in which the second layer starts to grow before the first layer is completed. This mode of growth is termed pseudo layer-by-layer. (c) We could also be observing Stranski-Krastanov growth mode. It is therefore not easy to distinguish the growth mode further without use of other experimental techniques to probe the surface morphology. We will attempt to resolve this observation by examining the surface morphology at various stages of growth using the AFM.

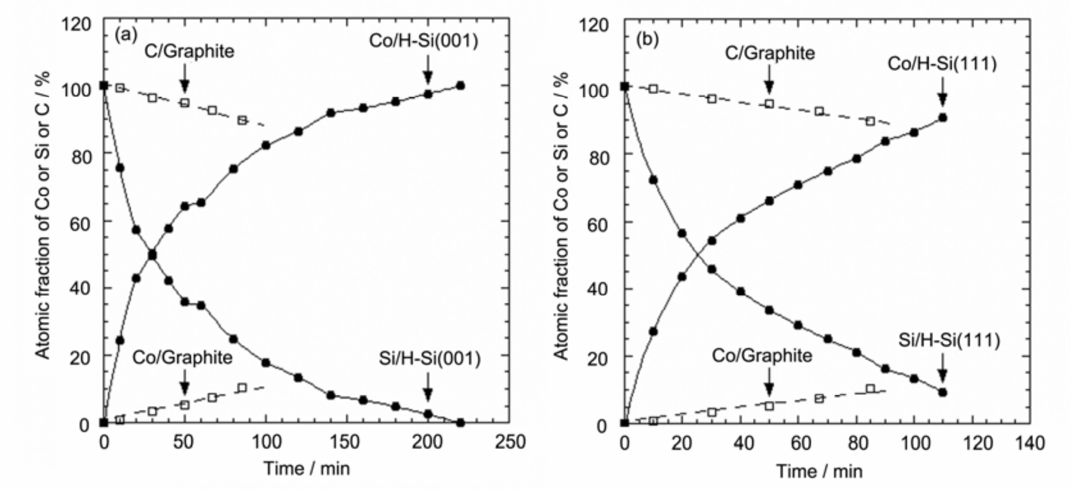

Fig.2 Evolution of the atomic fraction of Co and Si (represented in black circles) during Co evaporation on (a) H-Si(001) and (b) H-Si(111) surfaces. Un-shaded squares seen in the plots are data obtained for growth on Co on graphite surface.

The resulting morphology of the film following a pseudo layer-by-layer growth mode will likely to be flat and smooth. We will highlight the results obtained for H-Si(111) surface since the result for H-Si(001) is the same. Fig. 3 shows the AFM 1μm × 1μm scans taken of the surface with a Co coverage equivalent to atomic fractions of 5%, 15%, 25% and 50% on H-Si(111) surface. The surface morphology appears to be relatively featureless. The surface appears to be smooth and flat with a r.m.s. roughness of ~ 0.3nm. The observation of this smooth morphology is therefore consistent with a pseudo layer-by-layer growth mode on the H-terminated surfaces.

Fig. 4 shows the AFM 1μm × 1μm scans taken of the surface with a Co coverage equivalent to atomic fractions of 5%, 15%, 25% and 50% on clean Si(111) surface. The surface morphology is no longer featureless. We can observe formation of close-packed islands on the surface throughout the deposition process. The observation of these compact and fixed size islands at various stages of deposition seems to give rise to a growth mode equivalent to "layer-by-layer" growth of materials; i.e. the 2nd stack of islands does not grow until the 1st stack of islands has completely packed the initial surface. Similarly, the 3rd stacks of islands are not seen until the 2nd layer is fully covered by islands with dimension of ~20-30nm and height of 1.0-1.3nm. In doing so, there is no significant 3D growth. Moreover the formation of compact islands leaves little voids on the surface and a continuous film thus forms. An aspect ratio of 1:10 would also imply some significant wetting of the Si surface by Co during deposition. These factors thus make the distinction of growth mode by XPS between pseudo layer-by-layer and compact islands growth difficult. Without further AFM analysis, we would not have been able to realize there is a difference in the growth dynamics and morphology observed between clean and H-terminated Si surfaces.

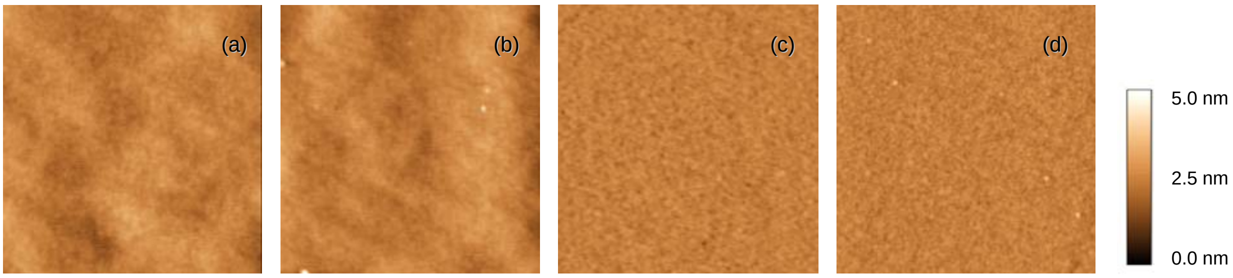

Fig.3 The 1μm × 1μm AFM images of various Co coverages equivalent to atomic fractions of (a) ~5%, (b) ~15%, (c) ~25% and (d) ~50% Co on H-terminated Si(111) surfaces at room temperature.

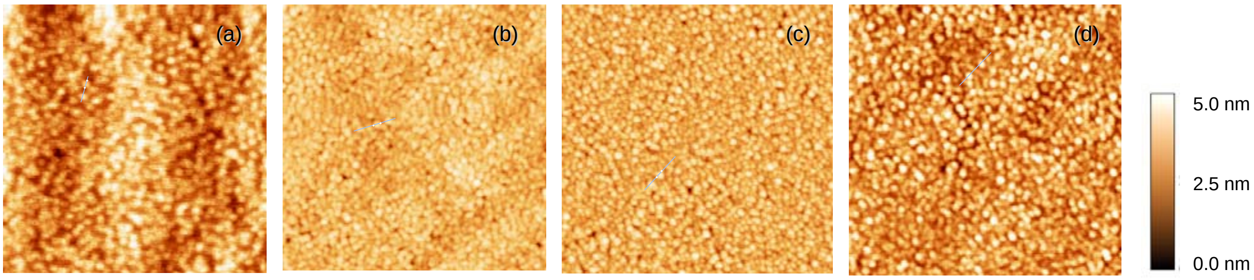

Fig.4 The 1μm × 1μm AFM images of various Co coverages equivalent to atomic fractions of (a) ~5%, (b) ~15%, (c) ~25% and (d) ~50% Co on clean Si(111) surfaces at room temperature.

3.3 Co diffusion behaviour during annealing of Co/Si interfaces

Fig. 5 shows the normalized ratio of the peak areas of Co $2p_{3/2}$ to Si 2p spectra as a function of annealing time. In the temperature range between RT and 200°C (300°C), this ratio is fairly constant and doesn't change significantly with annealing time on all four types of surfaces. However, a significant decrease in the ratio with time was observed when the sample was annealed to higher temperatures. For temperatures above 200°C-300°C, the decrease in the ratio with time shows qualitatively the same behavior on all four surfaces. Two regimes can clearly be identified. Regime 1 is characterized by an initial rapid decrease at the beginning of the annealing. This decrease in value however reaches a steady state in about ~12 min. The decrease in value is also more significant at higher temperature. Regime 2 on the other hand is characterized by a steady state value which only decreases with increasing annealing temperature. In order to explain the occurrence of regime 1 and more significantly regime 2, we consider the following possible scenarios.

(1) Co desorption from the surface. From the XPS data, the metallic "$CoSi_2$-like" film on Si is at least stable up to 200°C. Beyond that temperature, it may be possible that Co desorbs from the surface when temperature increases. Desorption is an activated process, hence more will be loss if heated to higher temperatures. While this may explain why the initial decrease in Co concentration is faster at higher temperature, it cannot account for the observation of a steady state value at a given temperature. In the event of an isothermal Co desorption, the concentration of Co should decrease and approach zero as time increases. It would not remain constant and only change when temperature is changed.

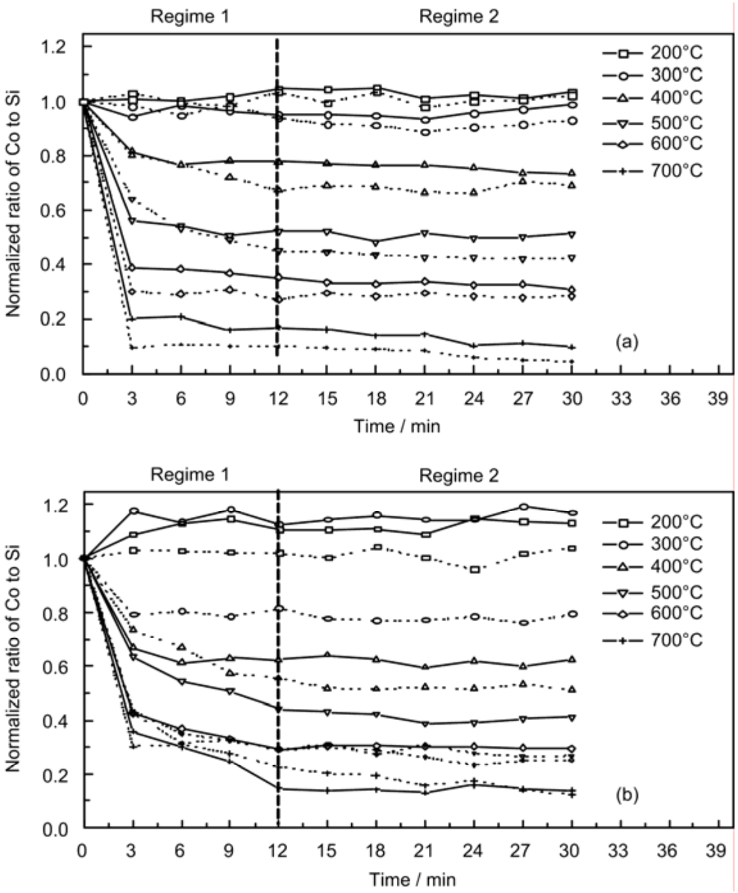

Fig.5 (a) and (b) show the normalized ratio of Co to Si versus annealing time at various temperature after ~5% Co deposited on clean and H-terminated Si(001) and Si(111) surfaces, respectively. Solid lines represent H-terminated Si surfaces while dotted lines represent the results on clean Si surfaces. The values shown in the plots are normalized to the initial ratio just before annealing, i.e. 5%.

(2) Simple Co inward diffusion or Si diffusion to the surface. It is possible for simple diffusion of Co atoms into the Si substrate as temperature increases. Similarly, Si may also diffuse from the substrate to the surface as temperature increases. Diffusion processes are strongly temperature dependent and it is also an activated process. The higher the temperature, the faster is the diffusion rate, and hence more Co is lost from the surface into the bulk or more Si moves to the surface depending which is the dominating diffusion process. While this can account for the occurrence of regime 1, the observation of a steady state value which does not change with time (i.e. regime 2) at a given temperature is harder to explain. More Co atoms from the surface will move into the semiconductor as the annealing time increases. Since a fixed amount of Co is deposited onto the semiconductor surface, the surface concentration will decrease as materials from the surface move into the bulk. Therefore the Co concentration within analysis depth of XPS will decrease and hence the relative ratio of Co/Si will not stay constant as the annealing time increases. This is again contrary to experimental observations. Similarly, if Si is the dominating diffusion species instead of Co, the same trend is expected.

(3) Diffusion and reaction of Co and Si to form silicides. Simple Co or Si diffusion cannot explain Fig. 5 and it is thus possible that there are other mechanisms operating. We have not, for example, considered the reaction between Co and Si atoms to form different silicide phases. This reaction is known to depend strongly on temperature and several possible Co-Si phases have been identified. When heated to ~ 250°C, Co and Si react to form a cobalt rich Co_2Si phase. This phase however is not stable at higher temperatures and further annealing to ~350°C leads to the formation of a highly resistive CoSi phase. By annealing to even higher temperatures, a silicon rich low resistive $CoSi_2$ phase forms at ~ 650°C. The stability of each phase is temperature dependent. Co_2Si phase for example is

more Co rich than CoSi and in turn is more Co rich than $CoSi_2$. Thus, it is possible that the steady state Co/Si ratio values at different temperatures are attributed to the stability and presence/coexistence of different Co-Si phases. The reaction of Co/Si to form Co_2Si, CoSi or $CoSi_2$ is an activated process and would also require Co atoms or Si atoms to diffuse through initial $CoSi_2$ layers to form more of these materials. The decrease in Co/Si ratio at higher temperatures could therefore be due to diffusion and phase transformation to a less Co rich or more Si rich silicide phase [31, 35]. In section 3.1, however, we found that there are no other silicide phases except the signature associated solely with $CoSi_2$. Therefore we conclude that reaction of Co and Si to form different silicide phases is not the reason.

(4) Surface morphological change (surface diffusion). Upon closer examination of Fig. 5, we find that the ratio of Co to Si on the surface is ~1:10 after annealing to 700°C. It is not the ratio of 1:2 as would be expected for formation of $CoSi_2$ films. This could imply that either the $CoSi_2$ film thus formed is very thin (less than XPS information depth) or it may not be continuous such that the underlying substrate Si or bare Si surface respectively is exposed and hence detected by XPS. An examination of the surface morphology before and after annealing is thus necessary. Fig. 6 shows the 4 μm × 4 μm AFM images of surface morphology for Co/H-terminated Si(001) and Si(111) surfaces prepared at room temperature and after annealing to various temperatures. While the initial surface is featureless, we found that the surface morphology after annealing is not. The Si(001) and Si(111) surfaces are observed to be covered by formation of rectangular and triangular silicide islands after annealing to higher temperatures respectively. Therefore the observed formation of $CoSi_2$ islands will expose more elemental Si atoms of the substrates within the XPS analysis depth compared to a flat thin film. In this case, apart from the decrease in Co signal due to inward diffusion, the overall Si 2p signal would also increase. These two effects will clearly decrease the intensity ratio of Co $2p_{3/2}$/Si 2p. With the density of islands decreasing as temperature increases, this would lead to a significant decrease in the normalized intensity ratios of Co $2p_{3/2}$/Si 2p. As a result, the initial decrease in the Co to Si ratio is more rapid at higher annealing temperature. Although not reported here, we have also observed that the density of islands at a given temperature do not change much once the annealing time exceeds 15 min. This observation could explain why a steady state (i.e. regime 2) is observed after an initial decrease occurs as described in Fig. 5.

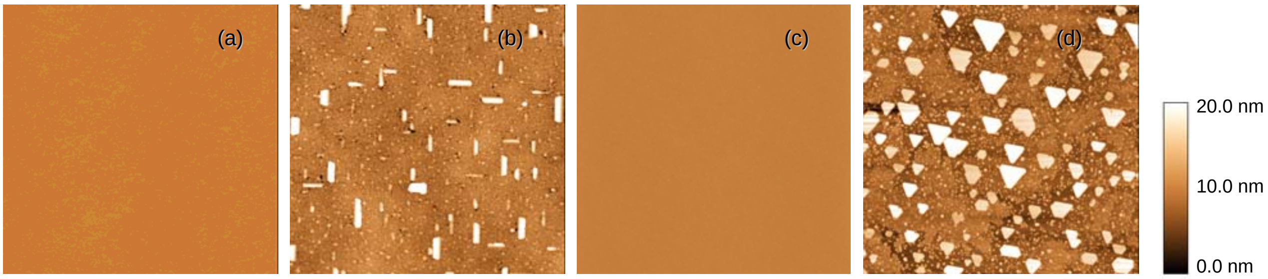

Fig.6 The 4 μm × 4 μm AFM images after annealing: (a) Co/H-terminated Si(001) surface to 300°C, (b) Co/H-terminated Si(001) surface to 700°C, (c) Co/H-terminated Si(111) surface to 300°C, and (d) Co/H-terminated Si(111) surface to 700°C.

4 Conclusions

It is evident from the above study that Co reacts strongly with the Si substrates to form a thin, amorphous $CoSi_2$-like layer at room temperature. This occurs on both clean and H-terminated Si surfaces. The presence of H-Si surfaces did not suppress the formation of the Co-silicide phase at room temperature. With further Co deposition, the interfacial layer composition becomes richer in Co and eventually a metallic Co film forms on top. XPS s-*t* curves appear to suggest that Co grows via a pseudo layer-by-layer mode on both clean and H-terminated Si surfaces. AFM images showed a smooth surface for Co deposition on H-terminated Si, while small close-packed island growth on the clean Si surface. H-termination appears to play a beneficial role for Co growth on Si surface. This effect has kinetic rather than energetic origin and appears to be a consequence of an increased surface diffusion rate of Co adatoms. The XPS s-*t* curve method was unable to distinguish between very closed-packed small island growth mode from pseudo layer-by-layer growth mode. Only $CoSi_2$ phase was observed during progressive annealing. This is different from a thick layer of Co deposited on Si substrate, a sequence of stable phases Co_2Si, CoSi and $CoSi_2$ was observed when they were annealed to different temperatures. The relative Co/Si ratio decreases with increasing annealing temperature, which is attributed to Co atoms inward diffusion and $CoSi_2$ island formation. The formation of $CoSi_2$ islands expose more elemental Si atoms of the substrate within the XPS analysis depth compared to a flat thin film, clearly decreasing the ratio of Co $2p_{3/2}$/Si 2p intensities. The Co/Si ratio shows similar trend on all four kinds of surfaces during annealing. Rectangular islands are formed on Si(001) surfaces while triangular islands are formed on Si(111) surfaces.

References

1 Tung R T. Mater. Chem. Phys., 1992, **32**: 107.

2 Von Känel H, Mater. Sci. Rep., 1992, **8**: 193.

3 Rathman D D. IEEE Trans. Electron Devices, 1990, **37**: 2090.

4 Levi A F J, Tung R T. Mater. Res. Soc. Symp. Proc. 1988, **102**: 361.

5 Maex K, Rossum M V. Properties of metal silicides, London: INSPEC Institute of Engineers, 1995.

6 Pirri C, Peruchetti J C, Gewinner G, *et al*. Phys. Rev. 1984, **B29**: 3391.

7 Boscherini F, Joyce J J, Ruckman M W, *et al*. Phys. Rev. 1987, **B35**: 4216.

8 Veuillen J Y, Nguyên T T A, Cinti R, *et al*. Phys. Rev. 1989, **B39**: 8015.

9 Meyerheim H L, Döbler U, Puschmann A. Phys. Rev., 1991, **B44**: 5738.

10 Nicolet M A, Lau S. S, VLSI microstructure science. Einspruch N G, Larrabee G B, Eds. New York: Academic Press, 1983.

11 Oura K, Lifshits V G, Saranin A A, *et al*. Surf. Sci. Rep. 1999, **35**: 1.

12 Murano K, Ueda K. Surf. Sci., 1996, **357-358** : 910.

13 Gergen B, Nienhaus H, Weinberg W H, *et al*. J. Vac.Sci. Technol., 2000, **B18**(5): 2401.

14 Tatsumura K, Watanabe T, Hara K, *et al*. Phys. Rev., 2001, **B64**: 115406.

15 Sumitomo K, Kobayashi T, Shoji F, *et al*. Phys. Rev. Lett., 1991, **66**: 1193.

16 Grupp C, Taleb-Ibrahimi A. Phys. Rev., 1998, **B57**: 6258.

17 Shen T C, Wang C, Tucker J R. Phys. Rev. Lett., 1997, **78**: 1271.

18 Grupp C, Taleb-lbrahimi A. J. Vac. Sci. Technol. 1998, **A16**(4): 2683.

19 Leisenberger F P, Ofner H, Ramsey M G, *et al*. Surf. Sci. 1997, **383**: 25.

20 Palasantzas G, Ilge B, de Nijs J, *et al*. Surf. Sci., 1998, **412/413**: 509.

21 Copel M, Tromp R M. Appl. Phys. Lett., 1994, **65**: 3102.

22 Gruyters M. Surf. Sci., 2002, **515**: 53.

23 Fritsch A, Legare P. Surf. Sci. 1984, **145**: L517; 1985, **162**:, 742.

24 Ma Q, Rosenberg R A. Surf. Sci., 1997, **391**: L1224.

25 Yang D Q, Sacher E. Surf. Sci., 2002, **504**: 125.

26 Diebold U, Pan J M, Madey T E. Phys. Rev., 1993, **B47**: 3868.

27 Mason M G, Phy. Rev., 1983, **B27**: 748.

28 Wertheim G K, di Cenzo S B. Phys. Rev., 1988, **B37**: 84.

29 Philips J M, Batsone J L, Hensel J C, *et al*. Appl. Phys. Lett., 1987, **51**: 1895.

30 Starke U, Weiss W, Rangelov G, *et al*. Surf. Sci., 1996, **352/354**: 89.

31 Ilge B, Palasantzas G, de Nijs J, *et al*. Surf. Sci., 1999, **414**: 279.

32 Gallego J M, Miranda R, Molodtsov S, *et al*. Surf. Sci., 1990, **239**: 203.

33 Copel M, Reuter M C, Kaxiaras E, *et al*. Phys. Rev. Lett. 1989, **63**: 632.

34 Hellman F, Tung R T. Phys. Rev., 1988, **B37**: 10786.

35 Kim K, Kang T H, Kim K, *et al*. Appl. Surf. Sci. 2000, **161**: 268.